

RESEARCH PAPER

## Polymer Flooding in a Heterogeneous Porous Media-Part II: A simulation Study

Seyed hosein Hayatolghheibi, Forough Ameli, Mohammad Reza Moghbeli\*, Mehdi Momenian

Smart Polymers and Nanocomposites Research Group, School of Chemical Engineering, Petroleum and Gas, Iran University of Science and Technology, Tehran 16846-13114, Iran

### ARTICLE INFO

Article History:

Received 4 April 2023

Revised 6 June 2023

Accepted 24 July 2023

Keywords:

AM/AMPS

Phase-field Model

Cahn-Hilliard equation

Non-homogeneous porous media

### ABSTRACT

The main goal of this study was to simulate the polymer injection test using the previously synthesized sulfonated acrylamide copolymer namely, acrylamide/2-acrylamido-2-methylpropane sulfonic acid (AM/AMPS). Phase-field approach was adopted for the simulation studies. Tuning parameters of this simulation study were interfacial tension ( $2 \times 10^{-6}$  N/m) and the contact surface thickness (0.305mm). The reported contact angle was  $40^\circ$  for the tuned model. Comsol Multiphysics software was used for the simulation. The selected polymer solution was prepared using equal ratios of AM and AMPS polymers, namely AMP55 with concentration of 2000 ppm and the injection test was conducted in micromodel. The recovery factor for the experimental and modeling studies, was reported as 26.91% and 29.4%, respectively, which represented a good agreement between the experimental and simulation studies. The effective injection test parameters on oil recovery factor for the polymer flooding experiments were investigated, including injection rate, copolymer solution viscosity, and the wettability of the porous media. The results were represented in a mathematical relation showing the relative effect of each parameter on the oil recovery factor.

### How to cite this article

Hayatolghheibi SH, Ameli F, Moghbeli MR, Momenian M., Polymer Flooding in a Heterogeneous Porous Media-Part II: A simulation Study, Journal of Oil, Gas and Petrochemical Technology, 2023; 10(1): 70-85. DOI:10.22034/jogpt.2023.391850.1118.

### 1. INTRODUCTION

Polymer flooding is regarded as a chemical enhanced oil recovery (EOR) technique for enhancing the recovery factor of conventional reservoirs with high mobility. One of the reasons for unstable flowing in heavy reservoirs is viscous fingering that would result in unstable displacement. Instability is augmented for the

heterogeneous reservoirs. This phenomenon is a function of injection flow rate, permeability, and water saturation. Polymer injection would lead to the reduction of the injected fluid mobility ratio. The stable flow occurs for the mobility ratios less than one.

The rheological behavior of polymer solutions may be affected by salinity and bivalent ion content. The effects of single-capacity and multi-capacity ions are different. Salinity is referred

\* Corresponding Author Email: [mr\\_moghbeli@iust.ac.ir](mailto:mr_moghbeli@iust.ac.ir)

to the total amount of anions. Ionic resistance is characterized by the concentration of ions in that solution. An increase in microscopic displacement efficiency in polymer flooding is the result of viscoelastic behavior of the polymer [1-6]. Some researchers have studied the modified structures of polymers with various degrees of hydrophobicity [7]. The most practical polymers that have been applied in EOR processes include polyacrylamide (PAM), hydrolyzed polyacrylamide (HPAM) and biopolymers such as Xanthan. Xanthan is produced by the fermentation of glucose using bacteria. This polymer is more resistant to brine in comparison to HPAM [8]. Other polymers include guar gum, sodium carboxymethyl cellulose, and hydroxyethyl ethyl cellulose [9]. Polyacrylamide is a synthetic polymer that is prepared by the polymerization of acrylic monomer to produce a polymer with flexible structure. The molecular weight of the commercial PAM is mainly in the range of  $5 \times 10^5$ – $5 \times 10^6$  g.mol<sup>-1</sup>, depending on the degree of polymerization [10]. PAM is strongly adsorbed on the surface of minerals. Therefore, this polymer is partially hydrolyzed to reduce the adsorption by reacting polyacrylamide with sodium hydroxide, potassium hydroxide or sodium carbonate. Hydroxide converts some amide groups (NH<sub>2</sub>) into carboxyl groups (COO<sup>-</sup>). The degree of hydration which is defined as a fraction of amidic groups and are converted by hydroxylation vary from 15% to 35% [11]. Hydrated polyacrylamide is actually a copolymer of acrylamide and acrylic acid. In fresh water, the repulsive force between carboxyl groups and polymer chains causes the chain stretching; consequently, the viscosity of polymer solution enhances. On the contrary, the chain collapse in saline or neutral water reduces the solution viscosity. Increasing the carboxylic groups in the polymer structure reduces the absorption of the polymer while increasing the viscosity.

Polymers including polyacrylamide (PAM) and partially hydrolyzed polyacrylamides (HPAM), are widely used in EOR processes, as the mobility enhancer. These polymers are not resistant to high salinity and temperature situations and cause viscosity and the oil recovery reduction. In these solutions, the present amide groups in the polymer solution are hydrolyzed to carboxylic groups which lead to the reaction with ions in the solution and reduction in the viscosity value. Precipitation would reduce the mobility

value and, in this way, block the pores and thus reduce the permeability. At high temperatures, the precipitation occurs more. The rheological properties of polymers would induce as a result of bridging due to the nanoparticles fluctuation. By combining the polyethylene (PEO) and polyacrylic acid (PAA) to silica nanoparticles, the polymers are adsorbed on nanoparticles to form a structure to enhance the suspension viscosity. By adding SiO<sub>2</sub> nanoparticles to locust bean gum (LBG) and xanthan gum (XG) and the combined gel (LX), the biopolymer properties change and the viscosity and elasticity of xanthan gum enhance [12].

Nanoparticles are applied for EOR processes. Nanopolymer suspensions were prepared using polyacrylamide as the polymer and silica as the nanoparticle [13]. The synthesized polymer showed higher viscosity in comparison to polyacrylamide. Surface nanoparticles were applied for the enhancement of recovery factor [14]. In a study by Corredor et al. [15], surface modified nanoparticles were applied for increasing the oil recovery factor. Adding SiO<sub>2</sub> nanoparticles to Xanthan gum led to mobility increase. Moreover, the capillary number also increased. However, they are not applicable in high salinity, high temperature, and high shear rates in which the polymer network is degraded and the recovery factor would reduce [16].

The application of Al<sub>2</sub>O<sub>3</sub> nanoparticles with polyacrylamide for EOR applications was studied by Gbadamosi et al. [17]. Adding this nanoparticle enhanced the recovery factor. The improvement of rheological properties of polymers was studied in laboratory. The measurement of hydrodynamic radius, phase behavior, and core displacement were performed in laboratory [18,19]. Druetta and Picchioni [20] performed a simulation study on the influence of nanoparticles on enhanced oil recovery of polymer flooding. Results indicated that this polymer flooding technique enhanced the %RF to 40-45%. Moreover, the synergic effect of nanoparticles and polymer would enhance the oil recovery factor [21].

Various techniques have been introduced for modeling the fluid flow in porous media including lattice Boltzmann [22-24], computational fluid dynamics [25,26] pore-network modeling [27,28], and statistical approaches [29]. For modeling the gas-liquid flow, finite volume approach was selected. It revealed that wettability and surface tension were the dominant flow mechanisms compared to gravity drainage. A comparison study

was performed between level set and phase field methods in terms of computation time and accuracy using Comsol Multiphysics.[30] Another study by Amiri and Hamouda [31] Comsol was used in water flooding process in a non-isothermal porous media. Effects of wettability, viscosity, capillary pressure, and heterogeneity were studied in pore level. Maaref et al. [32] investigated the effect of contact angle, viscosity, and heterogeneity on the

recovery factor. Their results showed low recovery factor in homogeneous porous media. Sinha et al. [33] simulated the flow of alkali-surfactant-polymer in porous media. The modeling results were compared with experimental data in terms of water cut and oil recovery factor. A comparison of advantages and disadvantages of different modeling methods is presented in Table 1 [34].

Table 1. Comparison of advantages and disadvantages of different modeling methods

Method	Advantages	Disadvantages
Front-tracking (FT)	Extremely accurate Robust Accounts for substantial topology changes in interface	Mapping of interface mesh onto Eulerian mesh Dynamic re-meshing required Merging and breakage of interfaces requires sub-grid model
Level set	Conceptually simple Easy to implement	Limited accuracy Loss of mass (volume)
Volume of fluid (VOF)	Relatively simple and accurate Easily adaptable to boundary fitted grids Merging and breakage of interface occurs automatically	Numerically diffusive Limited accuracy Extension to boundary fitted grids very difficult
Phase field	High capability in showing transport phenomena Ability to find the interface between three immiscible and incompressible phases Extremely accurate	Has large gradients that must be resolved computationally Thinness of interfacial layers Explicit discretization leads to numerical instability. Complexity in computational analysis
Lattice boltzmann	Perform all collisions in the simulation in one time step Low run time No numerical instability Easy to implement Automatically maintains sharp interfaces, and explicit interface tracking is not needed	The flow velocity cannot be high. Weakness in modeling gas-liquid multiphase flows with density difference or high viscosity difference between phases. Weakness in simulating streams with high Mach numbers. Weakness in modeling geometry with curved boundary.
Population balance model	Accurate No need for assumptions	Requires a lot of input data Time-consuming
Size exclusion	Suitable for modeling preformed particle gels	Cavernous occlusion Consider many hypotheses

The main goal of the present study was to perform a simulation study on a previously synthesized sulfonated acrylamide copolymer. The novelty of this work included the simulation of highly applicable polymer for the enhanced oil recovery process using Comsol Multiphysics software, and determining the tuning parameters of the model for a non-homogeneous glass micromodel. Moreover, effective parameters for the injection of the synthesized polymer in the glass micromodel were studied and introduced as a mathematical relation to be applied in similar conditions.

## 2. Materials and Methods

2-acrylamide-2-methylpropane sulfonic acid

(AMPS) was provided from Aldrich Co. Acrylamide (AM) monomer, methanol, acetone, potassium persulfate as initiator were provided from Merck Co., Germany. Heavy oil sample applied in this study was obtained from Bangestan reservoir in south of Iran. Oil interfacial tension and viscosity were 22.55 dyne/cm and 182cp, respectively. Viscosity values were measured by the Ostwald viscometry method. Physical properties of the oil sample and hydraulic properties of the micromodel are summarized in Table 2. Monomers were distilled under vacuum to eliminate the trace of inhibitors and then stored at 5°C. For polymer flooding studies, a glass micromodel was applied. Physical properties of the micromodel are shown in Table 3. Room temperature and pressure were

used for the tests with constant flow rate. The recovery factor and porosity of the system were calculated using the image processing of MATLAB Toolbox. Experimental set up is represented in Figure 1. A syringe pump (SPN1000HOM FNM) was used for the injection of the polymer into the

micromodel at constant rate of 0.0007 ml/min.

Table 2. Properties of the oil sample

Oil Viscosity (cp)	Interfacial Tension (dyne/cm)	Injection Rate (ml/min)
182	22.55	0.0007

Table 3. Properties of micromodel and oil sample

Pore Diameter (μm)	Throat Diameter (μm) (layer A)	Throat Diameter (μm) (Layer B)	Throat Diameter (μm) (layer C)	Average Aspect Ratio	Coordination Number	Porosity (%)	Etched Thickness (μm)
720	270	200	130	3.94	4	23	156

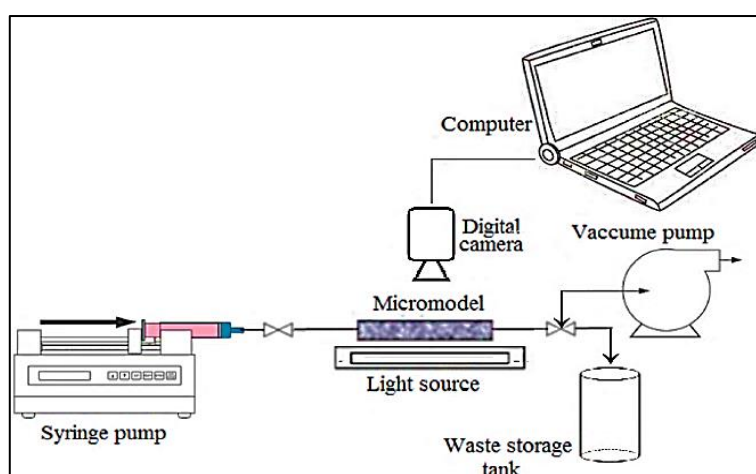


Figure 1. Schematic of the experimental set up

AM and AMPS copolymers were synthesized using the free radical polymerization method [35] in presence of a radical initiator in an aqueous medium. The prepared solution of two monomers were placed inside a four-span glass reactor at 25°C, and degassed with nitrogen for 20 minutes with agitator. Potassium persulfate was dissolved in 10cc of water with 0.1 molar ratio of monomer. Then it was degassed and heated to 60°C for 6 hrs. The final solution was a viscous and transparent liquid. At the end of the reaction, the solution was cooled to room temperature. A diagram for the polymerization process and reaction is shown in Figure 2.

### 2.1. Characterization

Viscosity of the prepared copolymer solutions with different concentrations was determined using Ostwald viscometry technique. The interfacial tension of the solutions was obtained using Pendant drop technique at 25°C.

### 2.2. Polymer Flooding Tests

As mentioned in the previous study, the synthesized copolymers functionality was investigated on the oil recovery factor using polymer injection tests. The Initial oil in place was obtained by the image processing of Matlab toolbox. The Injection rate of the polymer solution was 0.0007 ml min<sup>-1</sup>. The oil sweeping efficiency was obtained using the processing of the captured images during the oil sweeping at different time steps. Finally, the swept area was obtained to calculate the oil recovery factor.

### 3. Simulation Studies of Polymer Flooding

Comsol Multiphysics software was used to simulate polymer flooding experiments. For polymer injection tests, the selected polymer (PAM) solution was injected to micromodel with the flow rate of 0.0007 cc min<sup>-1</sup>. The concentration and viscosity of the polymer solution were 250 ppm and 1.09 cp, respectively.

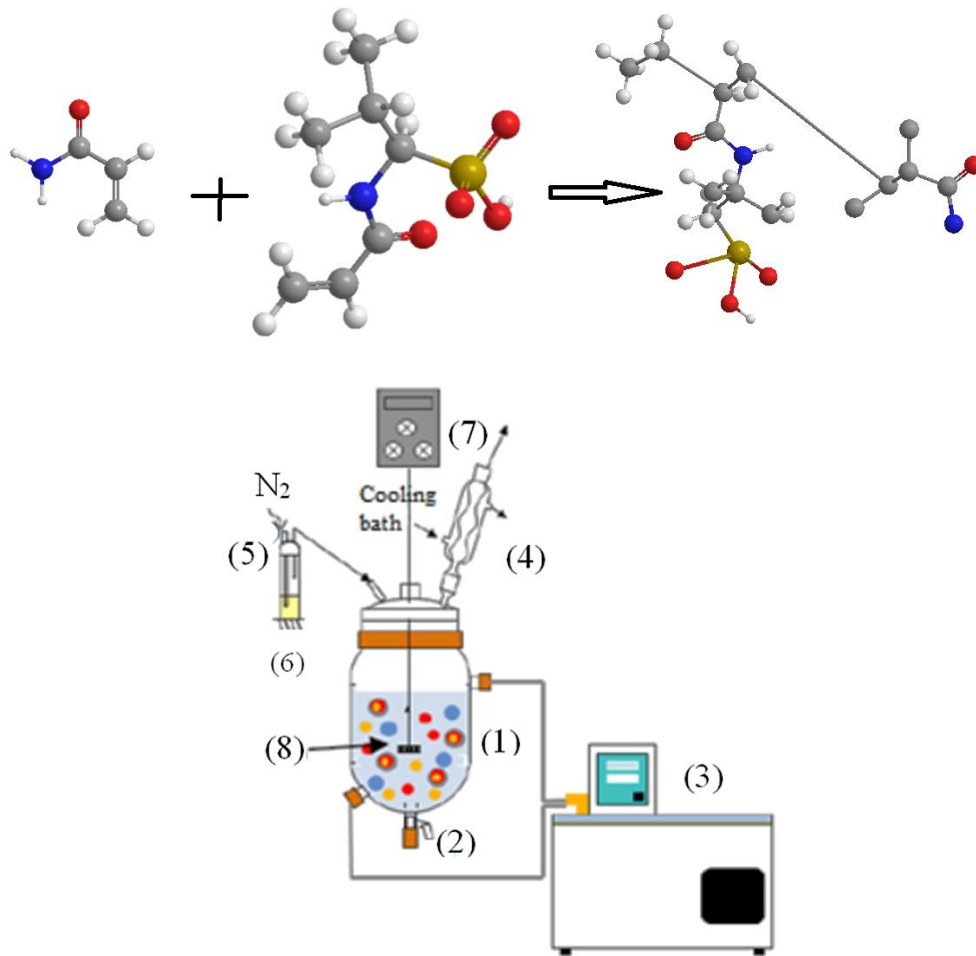


Figure 2. Schematic for the polymerization process and reaction

The following section illustrates the phase field approach used for the simulation of polymer flooding experiments.

### 3.1. Phase Field Model for Water and Polymer Flooding Tests

Application of phase-field model has significantly increased in recent years. The main property of this technique is defining a parameter changing along the contact surface and is constant in the phase environment. [36] The contact surface of the two phases is a thin layer which its diffusivity consists of two fluids. The transfer equations are established in contact surface of the two fluids. The chemical potential gradient is used to calculate the emission rate. Moreover, interfacial disturbance energy is used to determine the interfacial tension. [37] One of the most practical equations in phase-field modeling approach based on the work of Van der

Waals forces is Cahn-Hilliard equation. [38] In this approach, the equilibrium condition at surface is achieved for minimum free energy. This equation is given as follows:

$$\frac{\partial \phi}{\partial t} + \vec{u} \cdot \nabla \phi = \nabla \cdot M \nabla G \quad (1)$$

$\phi$  denotes the concentration fraction of the two components,  $M$  is the diffusion coefficient called mobility,  $G$  is the chemical potential of the system and  $u$  is velocity. The chemical potential of the system is represented as follows [37,39]:

$$G(\phi) = \lambda \left( \frac{\phi(\phi^2 - 1)}{\varepsilon^2} - \nabla^2 \phi \right) \quad (2)$$

here  $\lambda$  is the mixing energy density,  $\varepsilon$  is a capillary width that scales with the interface thickness. In this technique, density and viscosity

are determined as follows [37,39]:

$$\rho = \rho_1 v_{f1} + \rho_2 v_{f2} \quad (3)$$

$$\mu = \mu_1 V_{f1} + \mu_2 V_{f2} \quad (4)$$

$$v_{f1} = \frac{1 - \phi}{2} \cdot v_{f2} = \frac{1 + \phi}{2} \quad (5)$$

where  $\rho_1$  and  $\rho_2$ ,  $\mu_1$  and  $\mu_2$  represent the densities and viscosities of fluids 1 and 2, respectively. The fluids are incompressible which means mass and volume conservation laws are established.[40] Mean curvature ( $k$ ) is determined as follows [40]

$$k = 2(1 + \phi)(1 - \phi) \frac{G}{\sigma} \quad (6)$$

where  $\sigma$  denotes the surface tension. The precision analysis of this technique is performed by three factors including mobility, mesh size, and interface surface thickness. Turbulence and thickness of the boundary layers are controlled by mobility. This model is converged by combining phase field model approximation to real sharp surface and real solution of phase field model via numerical approaches.

For the three-phase flow, contact surface between the three immiscible incompressible phases is tracked. Navier-Stokes and continuity equations are solved and the contact surface of the fluids is detected by solving four equations for the chemical potential and phase field models. The contact surface of the fluids is moved by minimizing the free energy. Navier-Stoke equation is as follows [41]:

$$\rho \frac{\partial \vec{u}}{\partial t} + \rho(\vec{u} \cdot \nabla) \vec{u} = \nabla \cdot (-P + \mu(\nabla \vec{u} + \nabla \vec{u}^T) - \frac{2}{3} \mu(\nabla \cdot \vec{u})) + F_{st} \quad (7)$$

where  $p$  is pressure,  $F_{st}$  is surface tension represented as follows:

$$F_{st} = \sum_{ABC} \eta_i \nabla \phi_i \quad (8)$$

$$\eta_i = \frac{4 \sum_j \tau}{\epsilon} \sum_{j \neq i} \left( \frac{1}{\sum_j} \left( \frac{\partial F}{\partial \phi_i} - \frac{\partial F}{\partial \phi_j} \right) \right) - \frac{3}{4} \epsilon \sum_j \nabla^2 \phi_j \quad (9)$$

$\Sigma_i$  denotes the chemical potential of each phase.  $\epsilon$  represents control parameter for the contact surface thickness. The following equation is consistent for all the variables in phase field model.

$$\sum_{i=ABC} \phi_i = 1 \quad (10)$$

### 3.2. Boundary and Initial Conditions

In this study, finite element method was used to solve phase field equations using Comsol Multiphysics software (v.5.3). Boundary and initial conditions of the model are explained below.

#### • Inlet Boundary Conditions

The inlet boundary condition for micromodel is constant flow rate of 0.0007 ml/min. For phase field model, the fluid phases should be specified which are water for the two-phase flow and hydrogel solution for the three-phase flow.

#### • Outlet Boundary Condition

Outlet boundary condition is the atmospheric pressure.

#### • Walls

Walls are considered as solid impermeable surfaces with no slip boundary condition. Therefore, the fluid velocity on the wall would be non-slip and non-penetrating. The walls are impermeable.

$$u_f \cdot \hat{n} = 0 \quad (11)$$

$\hat{n}$  is the normal vector to the surface and the fluid velocities are equal at the interface ( $u_{f1} = u_{f2}$ ).

#### • Initial Conditions

The initial conditions are atmospheric pressure and ambient temperature. The initial condition for the phase field model is the saturation of the media with oil.

### 4. Results and Discussion

In this study, the results of the previous experimental study on the polymer injection test were used for the simulation study. The applied technique was the copolymerization of AM and AMPS monomers. The effects of the copolymer solution concentration and AM/AMPS ratio were investigated on the viscosity of the synthesized copolymer. The simulation study was conducted and the results were compared to the experimental data.

#### 4.1. Effect of Copolymer Solution concentration on the Viscosity

Viscosity of the solutions at different copolymer concentrations was determined using Ostwald viscometry technique. Based on the results, the

effect of the solutions was interpreted on their viscosities. The solutions were prepared at various copolymer concentrations of 0, 50, 500, 1000 and 2000 ppm. Ostwald viscometry technique was utilized to determine the solution viscosity. Results showed that an increase in the copolymer concentration led to the viscosity enhancement. Based on the results displayed in Figure 3, for all the polymers, viscosity of the aqueous solution increased by increasing the copolymer concentration. However, viscosity change was not the same for all the copolymers. Viscosity of 30cs for the copolymer concentration of 2000 ppm was obtained for AMP55 copolymer solution.

**4.1.1. Effect of Copolymer Composition on the Viscosity**

To evaluate the effect of AMPS content on the solution viscosity, different copolymer solutions were prepared and their viscosities were measured at the same concentrations. The viscometry results showed that increasing the AMPS up to 50% in the monomers feed, increased the solution viscosity to the highest value (Figure 4). However, further increase in AMPS content caused the viscosity decrement. As stated, the highest viscosity of the solution (30cs) belonged to the AMP55 solution while the lowest viscosity (5.3cs) was obtained for the AMP91 solution at the same copolymer concentration of 2000 ppm. The latter copolymer with the lowest AMPS content

(10wt.%) and the PAM solution without AMPS comonomer exhibited almost the same solution viscosity. This means that the addition of the lowest AM content had no significant effect on the PAM solution viscosity. The solution viscosity of 15.1 and 8cs was obtained for the AMP73 and AMP37 copolymers at the same copolymer concentration of 2000 ppm. It is obvious that the incorporation of the highest AMPS content (70 wt.%) in the AMP37 decreased the viscosity. For all the copolymers except for the AMP55, further increase of the copolymer concentration did not exert any significant effect on the solution viscosity. As shown in Figure 4, increasing the number of the hydrolyzed AMPS units in the copolymer chains, enhances the chain negative charges and subsequently, the solution viscosity. This behavior can be attributed to stretching of the chains in the aqueous solution by increasing the hydrolyzed 2-acrylamido-2methyl propane sulfonate (AMPA) units. In fact, the hydrodynamic volume of the chains and consequently the solution viscosity increased by increasing the AMPS content. On the other hand, due to excessive increase in the number of AMPS units in the chain, it is collapsed and twisted as a result of interlocked numerous ions with uneven loads of sodium. The resultant spiral shape and the decreased hydrodynamic volume would lead to the reduction of the solution viscosity.[42]

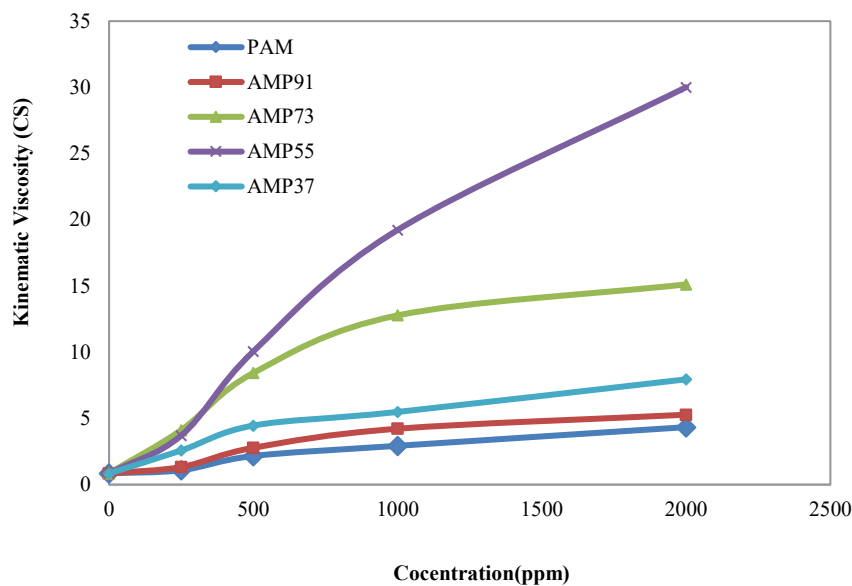


Figure 3. Viscosity of acrylamide copolymer at different concentrations of AM/AMPS at 28°C

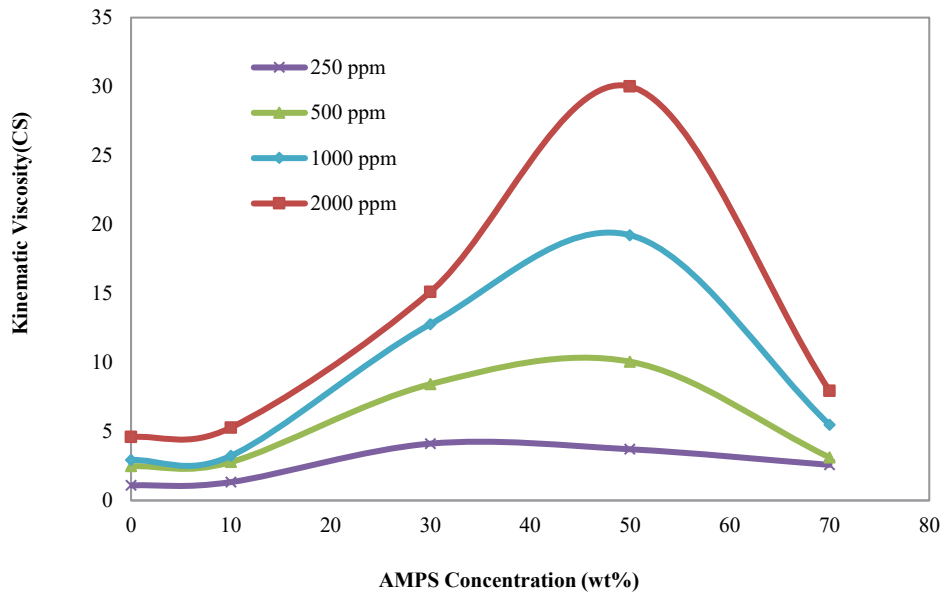


Figure 4. Viscosity of acrylamide copolymers in various AMPS concentrations at 28°C

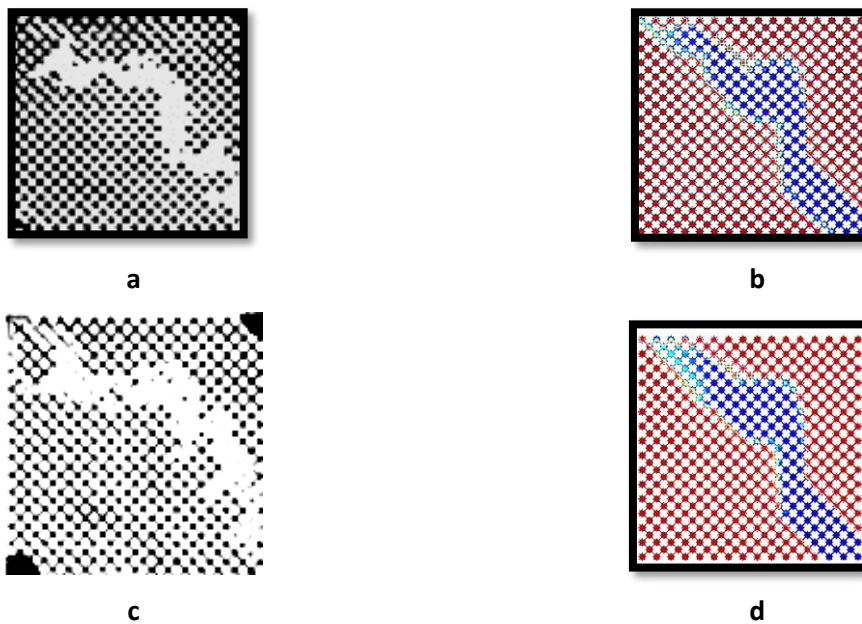


Figure 5. Comparison of experimental and modeling results for water flooding (a,b) and polymer flooding (c,d)

On the other hand, higher concentration of copolymer caused more chain entanglements and concentrated solution with higher viscosity.

#### 4.2. Polymer Flooding and Oil Recovery: Experimental Study

The experimental studies of the polymer injection tests are described in the previous works.

For the water flooding tests, since the viscosity of water is less than oil, the residual oil is not completely swept and fingering phenomenon is considerable. There are three different permeable layers in the prepared micromodel. The injected water first sweeps the high permeability region where the capillary forces are minimum. As a result, the fingering phenomenon pushes water toward

the production point. For the water flooding, the oil recovery factor was 18.7%. Increasing the synthesized copolymer concentration enhanced the oil recovery factor as a result of increasing the solution viscosity. Moreover, increasing the viscosity would reduce the solution mobility and the mobility ratio. The experimental studies revealed that AMP55 with concentration of 250 ppm enhanced the recovery factor from 7% to 26.91%. By duplicating the concentration of the copolymer, the oil recovery was reported to be 29.2%. For higher concentration values, the recovery factor slightly increased.

Moreover, the Polymer flooding tests were also performed using different concentrations of AMP73, including 250, 500, 1000, and 2000 ppm. Based on the results of the experimental studies, AMP55 represented the highest viscosity values, in comparison to other copolymers. There was no fingering phenomenon for the injection of AMP55, which led to high recovery factor. Moreover, increasing the concentration of the polymer solution enhanced the oil recovery factor considerably. For high values for the solution concentrations, i.e. 1000 and 2000 ppm, the RF sharply reduced.

#### 4.3. Polymer Flooding: Simulation Study

To perform polymer injection tests, the model was first saturated with oil. Then water was

injected with the flow rate of 0.0007 cc/min to sweep the oil. The thickness of the contact surface was considered as  $\frac{h_{max}}{1.8}$ , where  $h_{max}$  is the maximum mesh size equal to 0.55 mm. Interfacial tension of the two-phases was  $2 \times 10^{-6}$  N/m. Contact angle of  $40^\circ$  was obtained for the validated model for water sweeping. A comparison of the results for the simulation and the water flooding tests are shown in Figures 5a and 5b, respectively. As it is obvious, the modeling and experimental results are in good agreement. For water sweeping test, the recovery factor of 18.7% and 22.6% were obtained for the experimental and modeling results. After breakthrough time, the model was saturated with the oil, then the copolymer solution with concentration of 250 ppm was injected into the micromodel at flow rate of 0.0007 cc/min at  $28^\circ\text{C}$ . Viscosity of the polymer solution was reported to be 1.09 cp. The interfacial tension of the two phases and contact angel were  $2 \times 10^{-6}$  N/m and  $41^\circ$ , respectively. The experimental and modeling results for polymer flooding are represented in Figures 5c and 5d, respectively. As it is obvious from the figures, the modeling and experimental results agree well with each other. Experimental and modeling results for the RF were reported as 26.91% and 29.4%, respectively. The oil RF variation versus time is shown in Figure 6.

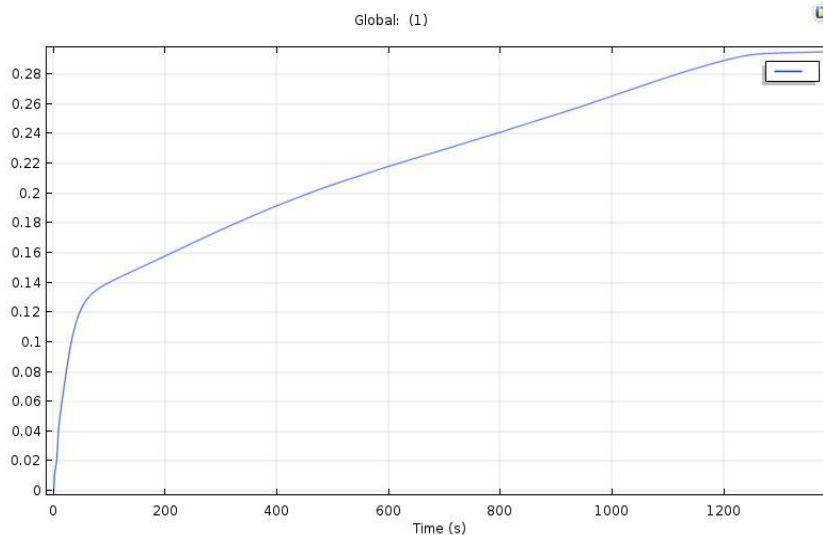


Figure 6. Variations of recovery factor with time

**4.3.1. Sensitivity Analysis**

After validation of the injection test results, the fluid and porous media parameters were changed to investigate their effect on the RF. Although the simulation results were not completely consistent with the field cases, it was possible to study the effect of each parameter on the results.

**4.3.1.1. Wettability**

In general, wettability is the degree to which a fluid tends to disperse on a solid surface in presence of other immiscible fluids. Wettability is one of the effective properties of the reservoir that significantly affects the recovery factor in EOR operations. Moreover, it is effective in identifying

the target reservoirs for EOR processes. Wettability is defined by the quantity of the contact angle. Figure 7a indicates the oil recovery factor for different contact angles at breakthrough time.

The RF optimal value of 29.8% was obtained at contact angle of 43°. By moving away from this optimal value, the RF reduced. For the water wet systems, the injected water would have a high tendency to move over the walls and form a thin layer. This issue may cause the formation of oil droplets inside the pores that are not recovered. By increasing the contact angle to 43°, more injected polymer solution entered to the pores to push the oil.

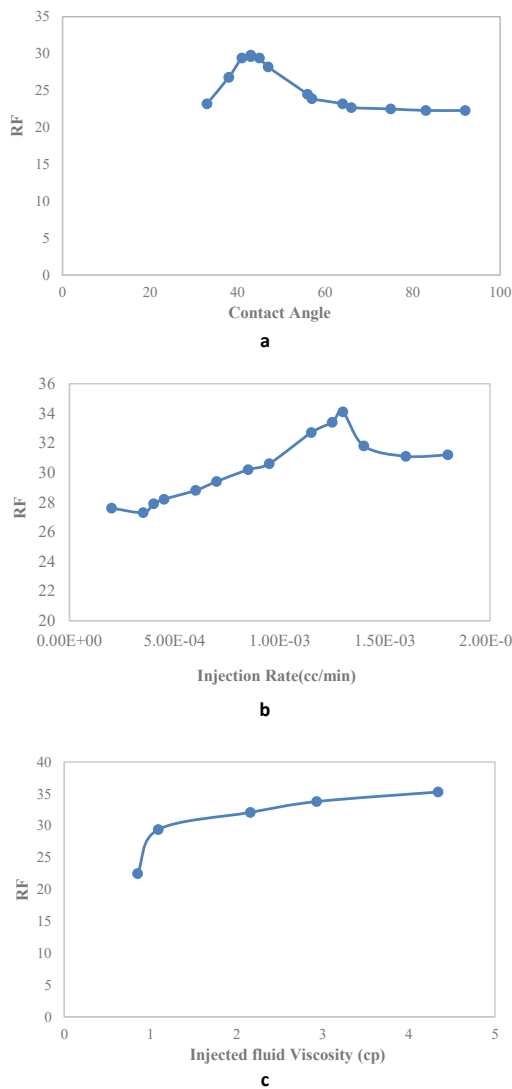


Figure 7. Oil recovery factor variations at a) Various contact angles at breakthrough time b) Various injection rates at breakthrough time c) Various injected fluid viscosity



In fact, at this contact angle, there was a tendency for water to move inside the large number of pores to sweep the available oil. As the contact angle increased, the tendency of the water for moving the oil near the surface of the micromodel reduced. This led to the reduction of the number of swept pores and, therefore, the RF value. Increasing the contact angle led to the reduction of the capillary force. This can decrease the tendency of the water for the oil sweeping in wet rocks. For large values of contact angle, the injected polymer solution moved in such a way that it reached to the production point from the shortest path with the least surface contact.

**4.3.1.2. Injection rate**

The fluid injection rate is another parameter that affects the recovery factor. As the injection rate increases, the viscous forces overcome the capillary ones. Thus, it increases the tendency of the fluid to pass through different channels and spread over a wider area of the micromodel. Injection rate is one of the parameters that has a significant impact on oil recovery factor. Figure 7b shows the RF variation for different injection rates at the breakthrough time. The proper recovery factor is obtained at the injection rate of 13e-3 cc/min, which is 34.1%. If the injection rate of the moving fluid deviates from this optimal value, the RF would decrease.

**4.3.1.3. Viscosity**

Viscous fingering depends on the viscosity ratio of the two fluids and the injection rate. By increasing the injection rate, the fluid velocity would increase and due to viscous fingering phenomenon, the sweeping of the fluid becomes non-uniform. In addition, the injected fluid leaves some areas unswept to reach to the production point. Mobility ratio (*M*) is one of the main concepts in studying the oil displacement by injecting the fluids such as water and polymers which is expressed as follows:

$$M = \frac{\lambda_o}{\lambda_w} = \frac{\frac{\mu_o}{k_w}}{\frac{\mu_w}{k_w}} \tag{12}$$

Where  $\lambda, k, \mu$  are the mobility, effective permeability and viscosity of the fluids, respectively. As the mobility ratio is decreased, displacement would be more uniform and the recovery factor would increase. In polymer flooding process, the focus is on reducing the mobility ratio. Increasing the viscosity of the injected fluid is one of the goals for increasing the recovery factor. Figure 7c represents the effect of the injected fluid viscosity on the recovery factor. As it is obvious in the figure, increasing the polymer solution viscosity (concentration) leads to increasing the RF.

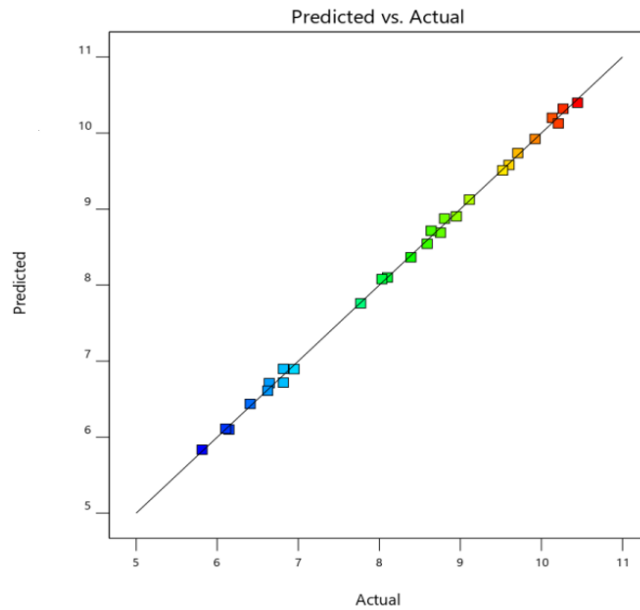


Figure 8. The proposed model predictions in comparison to the modeling results

Sensitivity analysis was performed on the three mentioned parameters including contact angle, injection rate and viscosity of the polymer solution. The last two terms are of crucial design parameters for the polymer flooding process, while contact angle is one of the important reservoir characteristics. These parameters were considered as the input variables for the statistical model. Analysis was performed using design expert software. The correlation between the recovery factor and these parameters is represented as follows:

$$RF^{0.62} = Aq + B\theta + C\mu + Dq\theta + E q\mu + F\theta\mu + Gq^2 + H\theta^2 + I\mu^2 + K \tag{13}$$

Where  $q$  is the injection rate,  $\mu$  represents the viscosity of polymer solution,  $\theta$  denotes the contact angle, and the coefficients of A to K are reported in Table 4. This equation in terms of actual factors can be used to make predictions about the response for given levels of each factor.

Table 4. Coefficient of the predicted model for sensitivity analysis on recovery factor

Parameter	value
K	+5.55648
A	+1434.86608
B	+0.012221
C	+0.025924
D	-0.207661
E	+0.059593
F	-0.000013
G	-4.65715E+05
H	-0.000137
I	-0.000045

This equation should not be used to determine the relative impact of each factor, because the coefficients are scaled to accommodate the units of each factor and the intercept is not at the center of the design space.

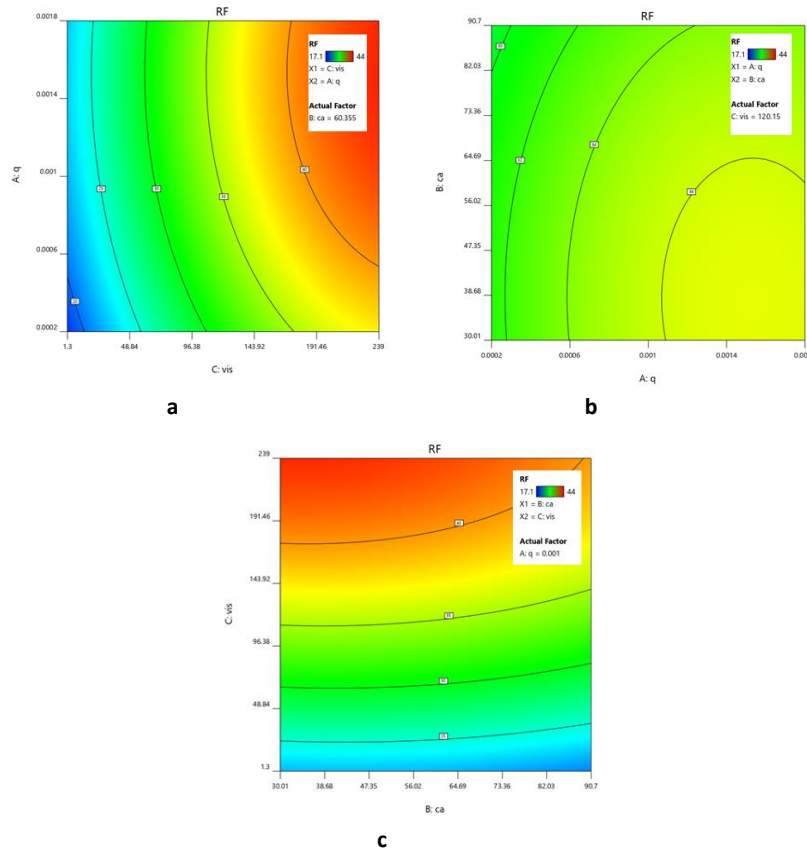


Figure 9. Combined effects the main polymer flooding parameters on oil RF, a) Injection Rate-Concentration b) Injection Rate-Contact Angle, c) Contact Angle-Concentration

Table 5. Results for ANOVA analysis

	Sum of Squares	df	Mean square	F-value	P-value
Model	56.36	9	6.26	1588.77	<0.0001
Residual	0.0670	17	0.0039		

Figure 8 illustrates the model prediction in comparison to the proposed modeling results. Most of the data are nested on the unit slope line. This means that the predicted model fits the data properly. ANOVA analysis of variance was performed for the experimental model to indicate its accuracy. The results are summarized in Table 5. F-value of the model indicates that it is significant. There is only 0.01% chance that such a large F-value is obtained due to the noise. P-values less than 0.05 indicate the consistency of the model. Figures 9a to 9c show the simultaneous effect of the two parameters on the oil recovery factor. As it is obvious in Figure 9a, the injection rate and viscosity have the most impact on oil recovery factor. Moreover, the wettability has the least effect on changing the oil recovery factor in comparison with the other two factors.

## 5. Conclusion

The main goal of this research was to conduct a simulation study on the injection of the previously synthesized sulfonated acrylamide copolymer, in the porous media. Moreover, the effect of copolymer composition and copolymer solution concentration, on the viscosity of the synthesized copolymer was studied. Based on the previous experimental study in a non-homogeneous porous media, the oil recovery factor was studied at various AM/AMPS ratios, copolymer solution concentration, and the silica nanoparticles. The results indicated that the RF value was four times than that of water injection test.

The main part of this study focused on the simulation of polymer flooding process using Comsol Multiphysics software by the application of phase-field model. The experiments led to the optimization of the synthesized copolymer composition to attain the maximum viscosity and oil sweeping efficiency. Experimental results were validated using Comsol Multiphysics for the water flooding and polymer flooding experiments with good accuracy were reported as 26.91% and 29.4%, respectively. Effective parameters of polymer injection tests, polymer solution viscosity, injection rate, and wettability of the porous media

were studied on the recovery factor. The results were represented in a mathematical relation showing the relative effects of each parameter on the oil recovery factor.

## Nomenclature

Physical Quantity	unit
Free Energy	J
Free Energy Density	J.m <sup>-3</sup>
Chemical Potential	J.m <sup>-3</sup>
Phase field ( $\phi$ )	-
Mobility (M)	J <sup>-1</sup> m <sup>5</sup> s <sup>-1</sup>
Surface Tension	N.m <sup>-1</sup>
Velocity	m.s <sup>-1</sup>
Pressure	Pa
Mass Density	Kg.m <sup>-3</sup>
Viscosity	Pa.s

## Author Contribution Statement

Mehdi Momenian: Formal analysis, Validation; Mohammad Reza Moghbeli: Supervision, Formal analysis Writing-Review & Editing; Forough Ameli: Writing-Original Draft, Data curation, Formal analysis; Seyed Hosein Hayatolghеibi: Formal analysis, Validation, Data curation

## Competing Interests

The authors declare no competing interests.

## References

- Huifen, X., Ye, J., Kong, F. & Wu, J. in *SPE Annual Technical Conference and Exhibition*. (Society of Petroleum Engineers).
- Jiang, H. et al. in *SPE Annual Technical Conference and Exhibition*. (Society of Petroleum Engineers).
- Wang, D. et al. in *SPE annual technical conference and exhibition*. (Society of Petroleum Engineers).
- Wang, D., Xia, H., Yang, S. & Wang, G. in *SPE EOR Conference at Oil & Gas West Asia*. (Society of Petroleum Engineers).
- Xia, H. et al. in *SPE Symposium on Improved Oil Recovery*. (Society of Petroleum Engineers).
- Yin, H., Wang, D. & Zhong, H. in *SPE Annual Technical Conference and Exhibition*. (Society of Petroleum Engineers).

7. Tripathi, A., Tam, K. C. & McKinley, G. H. Rheology and dynamics of associative polymers in shear and extension: theory and experiments. *Macromolecules* 39, 1981-1999 (2006).
8. Littmann, W. *Polymer flooding*. Vol. 24 (Elsevier, 1988).
9. Sheng, J. J. Chapter 7-Surfactant flooding. *Modern chemical enhanced oil recovery*. Boston: Gulf Professional Publishing, 239-335 (2011).
10. Willhite, G. P. & Dominguez, J. G. in *Improved oil recovery by surfactant and polymer flooding* 511-554 (Elsevier, 1977).
11. Abbas, S., Sanders, A. W. & Donovan, J. C. in *SPE Enhanced Oil Recovery Conference*. (Society of Petroleum Engineers).
12. Maurya, N. K. & Mandal, A. Studies on behavior of suspension of silica nanoparticle in aqueous polyacrylamide solution for application in enhanced oil recovery. *Petroleum Science and Technology* 34, 429-436 (2016).
13. Kennedy, J. R., Kent, K. E. & Brown, J. R. Rheology of dispersions of xanthan gum, locust bean gum and mixed biopolymer gel with silicon dioxide nanoparticles. *Materials Science and Engineering: C* 48, 347-353 (2015).
14. Pal, N., Kumar, S., Bera, A. & Mandal, A. Phase behaviour and characterization of microemulsion stabilized by a novel synthesized surfactant: Implications for enhanced oil recovery. *Fuel* 235, 995-1009 (2019).
15. Yousefvand, H. & Jafari, A. Enhanced oil recovery using polymer/nanosilica. *Procedia Materials Science* 11, 565-570 (2015).
16. Ghosh, P. & Mohanty, K. K. Study of surfactant-polymer flooding in high-temperature and high-salinity carbonate rocks. *Energy & Fuels* 33, 4130-4145 (2019).
17. Gbadamosi, A. O. et al. Effect of aluminium oxide nanoparticles on oilfield polyacrylamide: Rheology, interfacial tension, wettability and oil displacement studies. *Journal of Molecular Liquids* 296, 111863 (2019).
18. Orodu, K. B., Afolabi, R. O., Oluwasijuwomi, T. D. & Orodu, O. D. Effect of aluminum oxide nanoparticles on the rheology and stability of a biopolymer for enhanced oil recovery. *Journal of Molecular Liquids* 288, 110864 (2019).
19. Llanos, S. n., Giraldo, L. J., Santamaria, O., Franco, C. A. & Cortés, F. B. Effect of sodium oleate surfactant concentration grafted onto SiO<sub>2</sub> nanoparticles in polymer flooding processes. *ACS omega* 3, 18673-18684 (2018).
20. Druetta, P. & Picchioni, F. Polymer and nanoparticles flooding as a new method for Enhanced Oil Recovery. *Journal of petroleum science and engineering* 177, 479-495 (2019).
21. Bera, A., Shah, S., Shah, M., Agarwal, J. & Vij, R. K. Mechanistic study on silica nanoparticles-assisted guar gum polymer flooding for enhanced oil recovery in sandstone reservoirs. *Colloids and Surfaces A: Physicochemical and Engineering Aspects* 598, 124833 (2020).
22. Liu, Z. & Wu, H. Pore-scale modeling of immiscible two-phase flow in complex porous media. *Applied Thermal Engineering* 93, 1394-1402 (2016).
23. Huang, H., Huang, J.-J. & Lu, X.-Y. Study of immiscible displacements in porous media using a color-gradient-based multiphase lattice Boltzmann method. *Computers & Fluids* 93, 164-172 (2014).
24. Liu, H. et al. Multiphase lattice Boltzmann simulations for porous media applications. *Computational Geosciences* 20, 777-805 (2016).
25. Gunde, A. C., Bera, B. & Mitra, S. K. Investigation of water and CO<sub>2</sub> (carbon dioxide) flooding using micro-CT (micro-computed tomography) images of Berea sandstone core using finite element simulations. *Energy* 35, 5209-5216 (2010).
26. Raeini, A. Q., Blunt, M. J. & Bijeljic, B. Modelling two-phase flow in porous media at the pore scale using the volume-of-fluid method. *Journal of Computational Physics* 231, 5653-5668 (2012).
27. Al-Gharbi, M. S. & Blunt, M. J. Dynamic network modeling of two-phase drainage in porous media. *Physical Review E* 71, 016308 (2005).
28. Piri, M. & Blunt, M. J. Three-dimensional mixed-wet random pore-scale network modeling of two- and three-phase flow in porous media. I. Model description. *Physical Review E* 71, 026301 (2005).
29. Krol, M. M., Mumford, K. G., Johnson, R. L. & Sleep, B. E. Modeling discrete gas bubble formation and mobilization during subsurface heating of contaminated zones. *Advances in water resources* 34, 537-549 (2011).
30. Liu, Z. & Wu, H. Pore-scale study on flow and heat transfer in 3D reconstructed porous media using micro-tomography images. *Applied Thermal Engineering* 100, 602-610 (2016).
31. Amiri, H. A. & Hamouda, A. A. Evaluation of level set and phase field methods in modeling two phase flow with viscosity contrast through dual-permeability porous medium. *International Journal of Multiphase Flow* 52, 22-34 (2013).
32. Maaref, S., Rokhforouz, M. R. & Ayatollahi, S. Numerical investigation of two phase flow in micromodel porous media: Effects of wettability, heterogeneity, and viscosity. *The Canadian Journal of Chemical Engineering* 95, 1213-1223 (2017).
33. Sinha, A. K. et al. Numerical simulation of enhanced oil recovery by alkali-surfactant-polymer floodings. *Petroleum Science and Technology* 33, 1229-1237 (2015).
34. Gopala, V. R. & Van Wachem, B. G. Volume of fluid methods for immiscible-fluid and free-surface flows. *Chemical Engineering Journal* 141, 204-221 (2008).
35. Jamshidi, H. & Rabiee, A. Synthesis and characterization of acrylamide-based anionic copolymer and investigation of solution properties. *Advances in Materials Science and Engineering* 2014 (2014).
36. Badalassi, V., Cenicerros, H. & Banerjee, S. Computation of multiphase systems with phase field models. *Journal of computational physics* 190, 371-397 (2003).
37. Jacqmin, D. Calculation of Two-Phase Navier-Stokes Flows Using Phase-Field Modeling. *Journal of Computational Physics* 155, 96-127, doi:https://doi.org/10.1006/jcph.1999.6332 (1999).
38. Akhlaghi Amiri, H. A. in *COMSOL Conference 2014*.
39. Akhlaghi Amiri, H. A. & Hamouda, A. A. Evaluation of level set and phase field methods in modeling two phase flow with viscosity contrast through dual-permeability porous medium. *International Journal of Multiphase Flow* 52, 22-34, doi:https://doi.org/10.1016/j.ijmultiphaseflow.2012.12.006 (2013).
40. Yue, P., Zhou, C. & Feng, J. J. Spontaneous shrinkage of drops and mass conservation in phase-field simulations.

- Journal of Computational Physics* 223, 1-9, doi:https://doi.org/10.1016/j.jcp.2006.11.020 (2007).
41. Jafari, A., Hasani, M., Hosseini, M. & Gharibshahi, R. Application of CFD technique to simulate enhanced oil recovery processes: current status and future opportunities. *Petroleum Science* 17, 434-456 (2020).
42. Rabiee, A., Langroudi, A. E., Jamshidi, H. & Gilani, M. Preparation and Characterization of Hybrid Nanocomposite of Polyacrylamide/Silica-Nanoparticles. *Science and Technology* 25, 405-414 (2013).

## بررسی تزریق پلیمر در یک محیط متخلخل ناهمگون - بخش دوم: مطالعه شبیه سازی

سیدحسین حیات الغیبی، فروغ عاملی، محمدرضا مقبلی\*، مهدی مومنیان

گروه تحقیقاتی پلیمرهای هوشمند و نانوکامپوزیت ها، دانشکده مهندسی شیمی، نفت و گاز، دانشگاه علم و صنعت ایران،

تهران، صندوق پستی ۱۳۱۱۴-۱۶۸۴۶

### چکیده

هدف اصلی این مقاله، شبیه سازی تزریق کوپلیمر از پیش ساخته شده آکریل امید سولفوناته، با نام آکریل آمید/۲-آکریلامیدو-۲-متیل پروپان سولفونیک اسید (SPMA/MA) است. رویکرد میدانی-فازی برای مطالعات شبیه سازی مورد استفاده قرار گرفت. پارامترهای تنظیم شونده مدل در این مطالعه شامل کشش سطحی ( $10^{-6} \text{ m/N}$ ) و ضخامت مشترک ( $0.305 \text{ mm}$ ) می باشد. زاویه تماس در مدل تنظیم شده برابر ۴۰ درجه بدست آمد. برای شبیه سازی از نرم افزار کامسول استفاده گردید. محلول پلیمری انتخاب شده با استفاده از پلیمرهای MA و SPMA تهیه گردید و با غلظت ۲۰۰۰ mpp تست های میکرومدل انجام گرفت. ضریب بازیابی نفت در مدل تجربی و شبیه سازی به ترتیب معادل ۲۶.۹۱% و ۲۹.۴% بدست آمد که تطابق خوبی را بین مدل آزمایشگاهی و شبیه سازی نشان می دهد. پارامترهای موثر بر بازیابی نفت شامل سرعت تزریق، ویسکوزیته محلول پلیمری و ترشوندگی محیط در قالب یک مدل ریاضی ارائه گردید.

### مشخصات مقاله

#### تاریخچه مقاله:

دریافت: ۱۵ فروردین ۱۴۰۲

دریافت پس از اصلاح: ۱۶ خرداد ۱۴۰۲

پذیرش نهایی: ۲ مرداد ۱۴۰۲

کلمات کلیدی:

AM/AMPS

مدل میدانی-فازی

معادله کان-هیلیارد

محیط متخلخل ناهمگون

\*عهده دار مکاتبات: محمدرضا مقبلی

رایانامه:

mr\_moghbeli@iust.ac.ir

تلفن: ۰۲۱-۷۳۲۲۸۷۵۶

دورنگار: ۰۲۱-۷۷۲۴۰۴۹۵

نحوه استناد به این مقاله:

Hayatolghiebi SH, Ameli F, Moghbeli MR, Momenian M., Polymer Flooding in a Heterogeneous Porous Media-Part II: A simulation Study, Journal of Oil, Gas and Petrochemical Technology, 2023; 10(1): 70-85. DOI:10.22034/jogpt.2023.391850.1118.